ACS OMEGA

http://pubs.acs.org/journal/acsodf

Article

Experimental Study on the Ethanol-Assisted Catalytic Steam Reforming of Endothermic Hydrocarbon Fuel

Jiang Guo, Mingyu Gao, Zekun Zheng, and Lingyun Hou*

Cite This: *ACS Omega* 2023, 8, 6860−6868

Read Online

ACCESS | Metrics & More | Article Recommendations

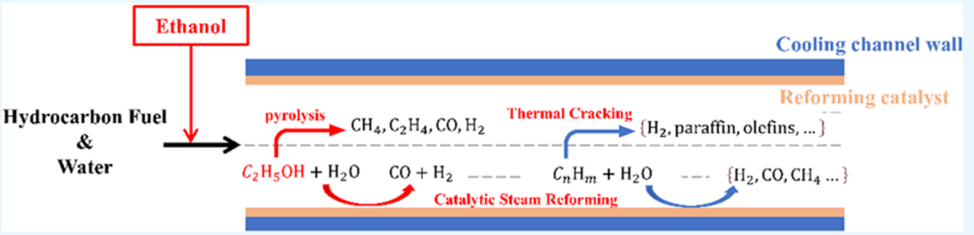

ABSTRACT: Thermal protection is a critical problem in the development of hypersonic aircraft. To enhance the thermal protection capability of hydrocarbon fuel, the ethanol-assisted catalytic steam reforming of endothermic hydrocarbon fuel was proposed. The result shows that the total heat sink can be significantly improved by the endothermic reactions of ethanol. A higher water/ethanol ratio can promote the steam reforming of ethanol and further increase the chemical heat sink. The addition of 10 wt % ethanol at 30 wt % water content can improve the total heat sink by 8−17% at 300−550 °C, which is caused by the heat absorption by phase transition and chemical reactions of ethanol. The reaction region of thermal cracking moves backward, resulting in the suppression of thermal cracking. Meanwhile, the addition of ethanol can inhibit the coke deposition and increase the working temperature upper limit of the active thermal protection.

1. INTRODUCTION

Engine thermal protection has become a critical problem for developing hypersonic aircraft. The demand for heat sink increases sharply with an increased flight Mach number.[1] Regenerative cooling with endothermic hydrocarbon fuel (EHF) is considered an effective way for engine thermal protection.[2] The cooling capacity of EHF consists of two parts: physical heat sink and chemical heat sink. The physical heat sink is decided by thermophysical properties, which are not sufficient for cooling demands and difficult to improve. The chemical heat sink comes from endothermic reactions. When the temperature reaches above 550 °C, the thermal cracking of fuel can provide a limited increase in cooling capacity.[3−5] To improve the fuel conversion rate and olefin selectivity in cracked products,[6,7] catalytic cracking of hydrocarbons is carried out to increase the chemical heat sink.[8−11] However, the initial temperature of cracking is high and is accompanied by severe coke deposition on the channel wall.[12,13] Thus, the temperature scope of fuel for regenerative cooling is limited.

Compared with thermal cracking, the catalytic steam reforming technology of hydrocarbon fuel with a strong endothermic capacity and low coking rate has attracted extensive attention.[14,15] In recent years, this technique has been investigated for the thermal protection of hypersonic aircraft. The excellent performance of the catalytic steam reforming technology has been proved by several experimental[16−20] and numerical[21−23] studies. However, the catalytic steam reforming reaction occurs over 450 °C,[19] meaning that the heat sink in the low-temperature section is still limited. Therefore, exploring new technology to improve the low-temperature heat sink release capacity of fuel is significant to improve the overall heat sink and broaden the scope of fuel use temperature.

Ethanol is an important renewable liquid fuel with a large latent heat of vaporization and an optimized combustion efficiency.[24] It is also an excellent organic solvent and miscible with hydrocarbon fuel. Significantly, the pyrolysis and steam reforming of ethanol can absorb a considerable amount of heat at a low temperature. Mason et al.[25] pointed out that ethanol can be dehydrated to ethylene at 270 °C. Zhang et al.[26] mentioned that when the temperature was above 240 °C, ethanol dehydration generated the main product of ethylene. Wang[27] proposed that among all of the decomposition reactions of ethanol, dehydration to ethylene is the main reaction pathway at low temperatures because of the lowest

Received: November 27, 2022
Accepted: January 27, 2023
Published: February 9, 2023

reaction energy barrier, which is consistent with the conclusion of Zhang et al. Steam reforming of ethanol (SRE) is an important approach for industrial hydrogen production.[28] Also, the SER process absorbs more heat compared with the pyrolysis of ethanol. Ni-based catalyst is the commonly used active metal because of its wide availability and low cost. It can promote the reforming reaction by breaking the C−C and C−H bonds.[29−31] Thermodynamic studies and sensitivity analysis[32−34] showed that the steam reforming of ethanol was feasible for temperatures higher than 500 K. Also, a higher water/ethanol ratio improved hydrogen selectivity and reduced coke deposition. Reaction models based on this analysis were proposed. Comas et al.[35] experimentally studied the SRE reaction with Ni/Al_2O_3 catalysis between 300 and 500 °C and indicated that a higher water/ethanol ratio (6:1) and higher temperature (500 °C) promoted hydrogen production. Therefore, the endothermic reactions of ethanol have a significant potential to assist regeneration cooling of hydrocarbon fuel.

There are only a few studies on ethanol-assisted regenerative cooling of hydrocarbon fuel. Gong et al.[36] found that when the volume ratio of ethanol to kerosene was 40%, ethanol addition promoted the production of H_2 and CO, which was a potential solution for the ignition and stable combustion challenge in scramjets. Xu et al.[37] found that the addition of ethanol to the RP-3 kerosene is beneficial to the enhancement of the overall heat sink for the endothermic process. The heat sink improvement mainly arose from the physical heat sink and dehydration of ethanol. Yang et al.[38] pointed out by experiment that carbon deposition in supercritical fuel cracking can be suppressed by adding 5 wt % ethanol to the RP-3 kerosene.

These studies only focus on the ethanol-assisted thermal cracking of fuel, but there is no relevant research on ethanol-assisted catalytic steam reforming of hydrocarbon fuel to make full use of the endothermic ability of SER. In this work, we introduced ethanol to the coupled thermal cracking and catalytic steam reforming of EHF to enhance the thermal protection capability. To do so, we have conducted a series of experimental studies of catalytic steam reforming based on a hydrocarbon fuel with a certain amount of ethanol addition. The characteristics of the heat sink, reaction conversions, heat transfer, and coke deposition in ethanol-assisted catalytic reforming of EHF were studied.

2. EXPERIMENTAL SYSTEM AND METHODS

The high-pressure test apparatus for the catalytic steam reforming is shown in Figure 1. The experimental setup consisted of a fuel supply and reaction, measurement, and sampling systems. The fuel supply system included a fuel tank, a filter, and a high-pressure liquid chromatography pump (Dalian Elite Analytical Instruments Co., Ltd.). The fuel used in the experiments was an endothermic hydrocarbon fuel (EHF), a specific China RP-3 fuel with carefully removed aromatics. It consisted mainly of paraffin (53.53 wt %) and cycloalkanes (46.09 wt %). The specific composition and properties are available in the previous literature.[16] Ethanol (99.7% pure, General-Reagent) had a critical pressure and temperature of 6.8 MPa and 243 °C, respectively. The EHF, water, and ethanol were mixed by a mechanical mixer to form an emulsion in the fuel tank and pumped into the reaction system by a high-pressure pump at a specific flow rate. The pump capacity was 20 MPa, and the flow rate limit was 500 mL/min with a measurement resolution of ±3%. A Coriolis mass flowmeter was used to measure the flow rate of the liquid fuel. The

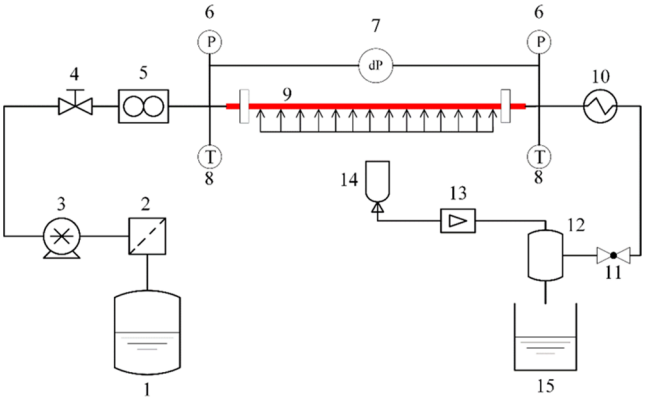

Figure 1. Experimental setup. 1: fuel tank; 2: filter; 3: high-pressure liquid chromatography pump; 4: valve; 5: mass flowmeter; 6: pressure gauge; 7: differential pressure sensor; 8: thermocouple; 9: reactor; 10: condenser; 11: back-pressure valve; 12: gas−liquid separator; 13: gas flowmeter; 14: airbag; 15: residual tank.

flowmeter capacity was 10 MPa, and the flow rate limit was 3 g/s with a measurement resolution of ±0.2%. The fuel supply delivery was stable and uniform to the subsequent heating and sampling sections.

Rectangular section tubes with inner dimensions of 3 mm × 2 mm and a length of 1200 mm were used as the reactor. These tubes were made of a high-temperature alloy, GH3128. The inner wall was coated with the Ni/Al_2O_3 reforming catalyst by plasma spraying. The thickness of the catalyst layer was controlled between 0.16 and 0.18 mm. The detailed properties of the catalyst layer are available in the previous literature.[16] Two copper boards at both ends of the reactor served as electrodes, and the reaction section tube between them was heated by a direct-current stabilized power supply. The power supply was controlled to provide different input powers by adjusting the constant current during the experiment, and the fuel that flowed through the channel was heated resistively. Two K-type thermocouples (0.2% accuracy) were placed at both ends of the reactor to measure the inlet and outlet fuel temperatures. The outer wall temperatures were measured by 14 K-type thermocouples that were welded outside the reactor surface.

Most heat was absorbed by the fuel, which promoted endothermic reactions. A small portion of the heat was dissipated to the environment by heat loss. The total heat sink (Δh_T) represents the endothermic ability of the fuel. It can be calculated as follows

$$\Delta h_T = (P - Q_{loss})/\dot{m}_{in} \quad (1)$$

where P is the input heating power of the reactor, $\dot{m}_{in}$ is the inlet mass flow rate, and Q_{loss} is the heat loss of the experimental setup, which can be calibrated using the dry heating method without fuel flow.

The total heat sink (Δh_T) takes both the physical heat sink (Δh_P) and the chemical heat sink (Δh_C) into account. The surrogated fuel model proposed in our previous studies[22] was used to determine the physical heat sink, which was calculated from the enthalpy changes between the inlet and outlet fuel temperatures. The chemical heat sink is the endothermic heat sink of the fuel thermal cracking and/or catalytic reactions, which is difficult to measure directly because of the complicated reaction processes. It can be obtained as follows

https://doi.org/10.1021/acsomega.2c07582
ACS Omega 2023, 8, 6860−6868

$$\Delta h_C = \Delta h_T - \Delta h_p \quad (2)$$

The product analysis system included the condenser, back-pressure valve, gas−liquid separator, and product-collection device. The fuel was condensed and the gaseous and liquid products were separated by the gas−liquid separator and sampled for analysis. The liquid and gaseous samples were analyzed quantitatively by gas chromatography−mass spectrometry (GC-MS DSQ, Thermo Fisher Scientific Inc.) and gas chromatography/thermal conductivity detectors (GC-TCD, Agilent Inc.), respectively. The gaseous products were mainly composed of H_2, CO, CO_2, C1−C4 alkanes, and alkenes. As for the composition of the liquid products, more than 100 species were identified. The compounds can be sorted into five groups based on their chemical structures, namely, paraffin, cycloalkanes, olefins, monocyclic aromatic hydrocarbons (MAHs), and polycyclic aromatic hydrocarbons (PAHs).

Coke formation is inevitable during thermal cracking at high temperatures. The coke deposits on the inner surface may cause the deterioration of heat transfer or block the tube. In this study, the coking rates of typical cases were measured by the temperature-programmed oxidation (TPO) method from 20 to 650 °C for 30 min. Detailed information on the TPO method can be found in our previous work.[16] Assuming that the main component of coke deposits is carbon,[39] the coking rate can be calculated as follows

$$\omega_{coke} = m_{coke}/(S_{in}t_{exp}) \quad (3)$$

where m_{coke} is the mass of coke, S_{in} is the inner area of the tube, and t_{exp} is the duration of the experiment.

The system pressure was regulated by the back-pressure valve. A differential pressure sensor (ROSEMONT 3051S) was placed at the end of the reactor to measure the pressure difference between the inlet and outlet. When the pressure difference between the two tips of the reaction tube exceeded 60 kPa, which indicated that the internal coking was severe, the experiment was stopped immediately. Prior to each test, nitrogen was used to purge the reactor channel. All parameters were logged on a computer. The experiment was executed as in our previous work.[12,16−19]

Seven cases were experimentally investigated and compared, as shown in Table 1. Case 1 referred to pure EHF using a bare tube without a catalyst. As a common regenerative cooling method without steam reforming, only thermal cracking of EHF occurred in case 1. Cases 2, 4, and 6 referred to EHF with different water contents using tubes with reforming catalysts. The water content of each group increased sequentially from 10 to 30 wt %. Cases 3, 5, and 7 added 10 wt % ethanol based on cases 2, 4, and 6, respectively. Cases 2 and 3, 4 and 5, 6 and 7 as three groups investigated the effect of ethanol addition on catalytic steam reforming of EHF. Cases 3, 5, and 7 investigated the effect of ethanol addition with different water contents. All cases were conducted under a critical pressure of 3 MPa with a feedstock flow rate of 1 g/s, and the inlet fuel temperature of the reactor was controlled at 20 °C.

Table 1. Experimental Cases

		mass fraction (wt %)		
cases	tube	EHF	water	ethanol
1	bare	100	0	0
2	catalytic	90	10	0
3	catalytic	80	10	10
4	catalytic	80	20	0
5	catalytic	70	20	10
6	catalytic	70	30	0
7	catalytic	60	30	10

3. RESULTS AND DISCUSSION

3.1. Characteristics of the Heat Sink. As shown in Figure 2, the total heat sinks of cases 2, 4, and 6 are all higher than that of case 1 over the entire temperature range, which is caused by the higher physical enthalpy of water and the promotion of the EHF steam reforming reaction.[18,22] On this basis, 10% ethanol is further added as in cases 3, 5, and 7. The differences in total heat sink indicate that ethanol addition affects the heat transfer in the tubes and is related to water content, which is analyzed in detail below. To facilitate analysis, the curve is divided into four zones according to the change of total heat sink with the outlet temperature, namely, the physical endothermic zone A, the ethanol reactions zone B, the transition zone C, and the EHF reactions zone D.

In zone A with the outlet temperature below 300 °C, the total heat sink is slightly increased with ethanol addition. Because in this temperature range, the heat absorption is basically derived from enthalpy change, and the enthalpy change of ethanol is higher than that of EHF. Moreover, the rapid increase in the total heat sinks at 200−250 °C is due to the phase change of ethanol and water. As the outlet temperature increases from 300 to 450 °C in zone B, the total heat sink is significantly improved by ethanol addition. According to the previous research,[19] the catalytic steam reforming of EHF occurs until 450 °C. Thus, it can be concluded that the endothermic reactions are only related to ethanol. There is already a certain amount of chemical heat sink at 300 °C due to the pyrolysis and steam reforming reactions of ethanol as shown in Figure 3. Therefore, zone B is the ethanol reactions zone. Also, higher water content further increases the chemical heat sink. In case 7 with 30 wt % water content, the total heat sink increases up to 8−17%.

However, the increment decreases at 450−550 °C in zone C. The total heat sink overlaps at about 550 °C, creating a turning point. In zone D with the outlet temperature above 550 °C, the total heat sink improves quickly but becomes slightly lower than the no ethanol addition cases under the same water content. For example, at 650 °C, the total heat sink of cases 5 and 7 decreased by 0.119 and 0.127 MJ/kg compared with cases 4 and 6, respectively.

The mechanism of ethanol addition effects on the total heat sink curves above 300 °C can be found by analyzing and quantifying the gaseous products and residual liquid components.

3.2. Reaction Mechanism. In zone B, as mentioned above, endothermic reactions of ethanol occurred. Gaseous products can be detected starting from 300 °C with a low generation rate, while there is no gaseous product in cases without ethanol addition. No ethanol is detected in the liquid products.

According to the research,[40−44] ethanol is easily hydrolyzed to ethylene at low temperatures. As the temperature rises, ethanol can be directly pyrolyzed into methane, carbon monoxide, and hydrogen, Meanwhile, the steam reforming processes of ethanol accompanied by the water-gas shift (WGS) reaction also occur. The reaction paths of ethanol pyrolysis and steam reforming can be summarized as follows

https://doi.org/10.1021/acsomega.2c07582
ACS Omega 2023, 8, 6860−6868

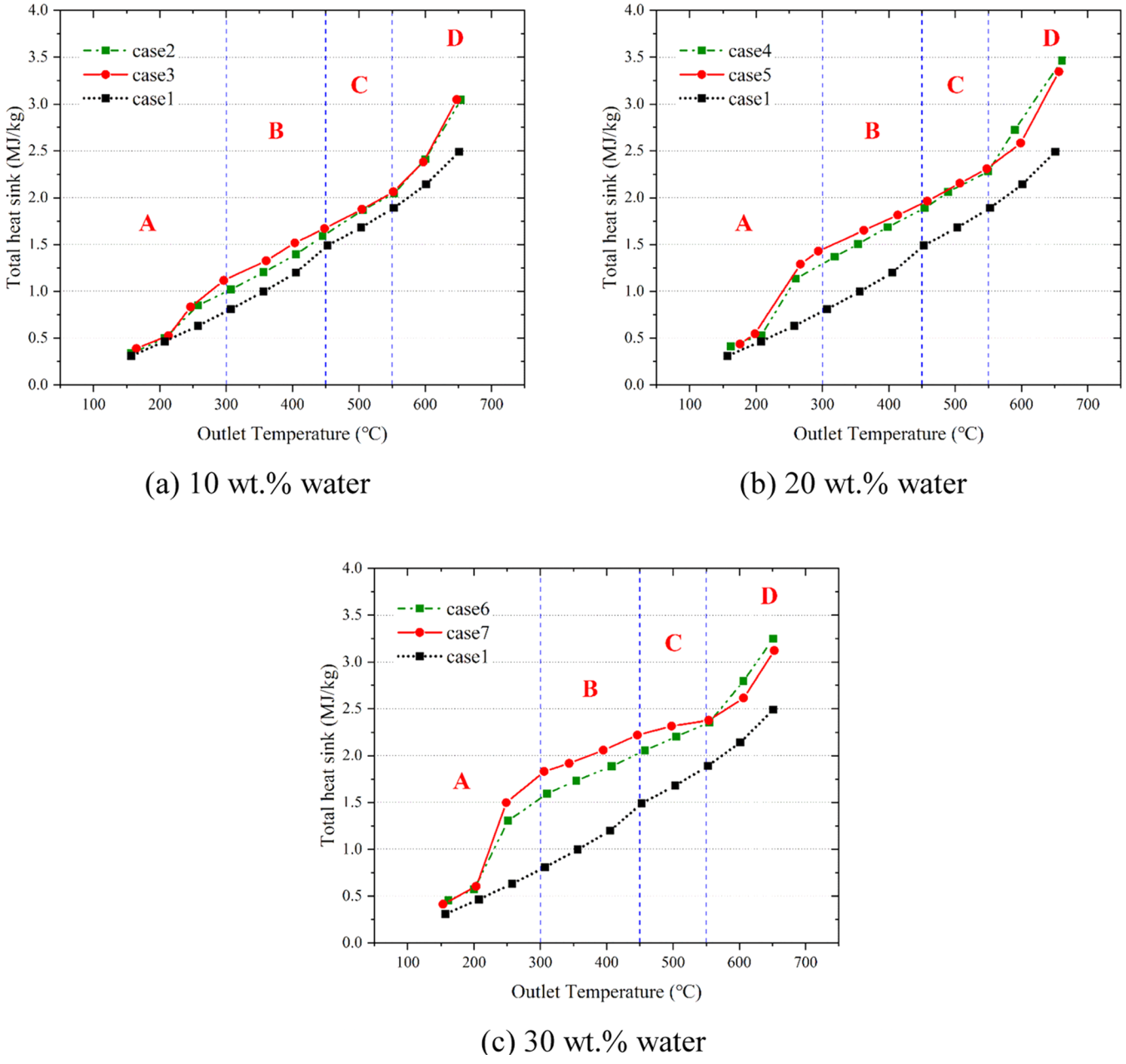

Figure 2. Total heat sink of ethanol addition with different water contents: A: physical endothermic zone; B: ethanol reactions zone; C: transition zone; D: EHF reactions zone.

$$C_2H_5OH \rightarrow C_2H_4 + H_2O, \quad \Delta H_{25}^0 = 45.5 \text{ kJ/mol} \tag{4}$$

$$C_2H_5OH \rightarrow CH_4 + CO + H_2, \quad \Delta H_{25}^0 = 49.6 \text{ kJ/mol} \tag{5}$$

$$C_2H_5OH + H_2O \rightarrow 2CO + 4H_2, \quad \Delta H_{25}^0 = 255.7 \text{ kJ/mol} \tag{6}$$

$$CO + H_2O \leftrightarrow CO_2 + H_2, \quad \Delta H_{25}^0 = -41.2 \text{ kJ/mol} \tag{7}$$

As illustrated in Figure 4, the gaseous products at 300 °C are composed of H_2, CO, CO_2, CH_4, and C_2H_4. According to eqs 4−7, H_2 is produced in every step of the reaction except eq 4, thus the mole fraction of H_2 in gaseous products can be up to 41−78%. CO is mainly from the SRE reaction and can be converted to CO_2 by the WGS reaction. CH_4 comes from ethanol decomposition. C_2H_4 is produced by the dehydration of ethanol. Therefore, the mole fraction of CH_4 and C_2H_4 can reflect the change in the proportion of ethanol pyrolysis. The mole fraction of CO is lower in each case because the SRE reaction can only occur on the catalyst surface at the wall. However, due to the highly endothermic character, the total heat sinks are still improved by ethanol addition in zone B.

As the water content increases, more H_2 and CO are detected and CO_2 fluctuates slightly, while the mole fractions of CH_4 and C_2H_4 decrease. This is because a higher water/ethanol ratio can improve hydrogen selectivity and promote SRE reaction.[33−35] The reductions of CH_4 and C_2H_4 indicate that the proportion of ethanol decomposition decreases. In conclusion, the higher water content can further increase the chemical heat sink in zone B.

When the temperature is above 450 °C, the catalytic steam reforming of hydrocarbon fuel takes place on the catalytic

https://doi.org/10.1021/acsomega.2c07582
ACS Omega 2023, 8, 6860−6868

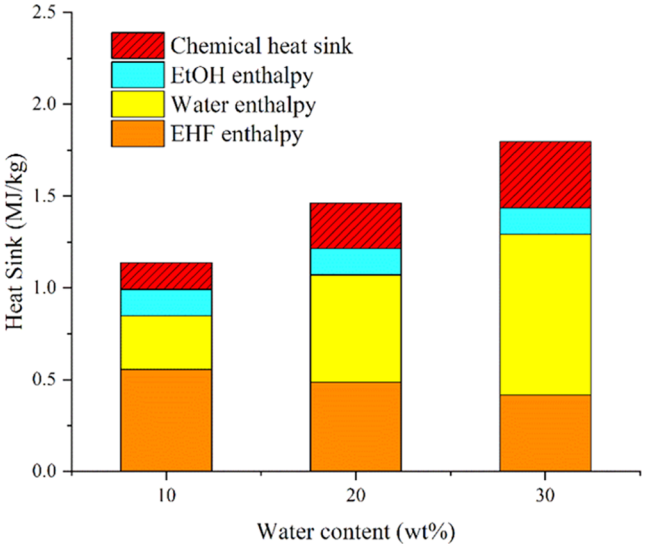

Figure 3. Comparison of the physical and chemical heat sinks of each component at 300 °C.

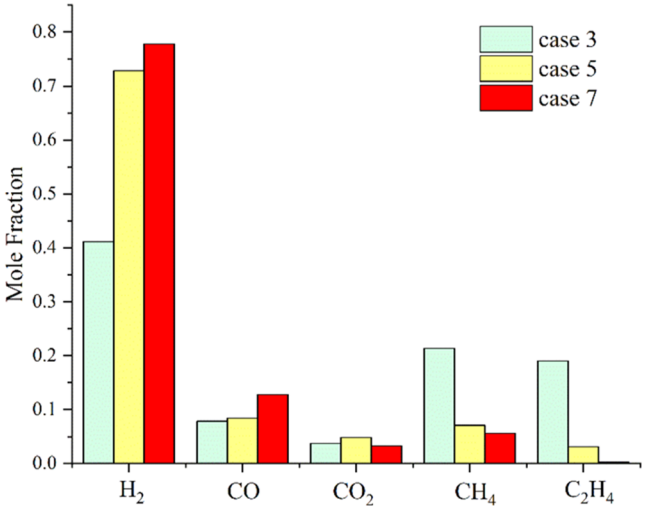

Figure 4. Comparison of gaseous products at 300 °C.

surface. The C−H bonds in the fuel and the H−O bonds in steam are broken and reformed into hydrogen, carbon monoxide, and low-molecular-weight hydrocarbons, shown as follows

$$C_nH_m + H_2O \rightarrow \{H_2, CO, CH_4, \cdots\} \quad (8)$$

Above 550 °C, the fuel thermal cracking reaction occurs and can be described as

$$C_nH_m \rightarrow \{H_2, \text{paraffin, olefins, } \cdots\} \quad (9)$$

In zone C, with the outlet temperature between 450 and 550 °C, the main reactant of the endothermic reaction is transferred from ethanol to EHF. Therefore, the transitional change in the total heat sink curves is due to the complex coupling of individual reactions in the reactor.

In zone D, as the temperature rises, thermal cracking of EHF takes place violently, resulting in the light hydrocarbons becoming the major gaseous products. With or without the ethanol addition, there is no difference in the species of components in the liquid product, only the mass fraction of each component changes. As illustrated in Figure 5a, with ethanol addition, the mole fraction of light hydrocarbons in gaseous products decreases slightly, while the mole fraction of H_2 and CO increases due to the ethanol reactions. Meanwhile, as the main components of the initial EHF, the increase of paraffin and cycloalkanes in Figure 5b indicates that the conversion of EHF is reduced. As shown in Figure 6, 10 wt % ethanol addition results in about a 33−42% reduction in fuel conversion, thus the heat sink is slightly lower than in the case of no addition of ethanol at the same water content. By contrast, the mass fraction of olefins and aromatics decreases. Also, almost no PAHs were detected in the cases with ethanol addition. Take the cases with 30 wt % water as an example, the mass fraction of MAHs reduces from 12.08 to 3.46% with 10 wt % ethanol addition, which is a relative decrease of 71.35%. The content of PAHs is close to 0. These differences between product distributions reflect the inhibition of EHF thermal cracking by ethanol addition.

As the water content increases, the mole fractions of H_2 and CO slightly increase, indicating that the steam reforming reactions of EHF and ethanol are promoted. The decrease in mass fraction of paraffin and cycloalkanes shows that the increase in the water content has an enhanced inhibitory effect on the EHF thermal cracking, thus increasing the fuel conversion.

According to the above analysis, the main reactions of ethanol-assisted catalytic steam reforming of EHF change with temperature in the cooling channel as shown in Figure 7. When the near-wall temperature reaches the ethanol reaction zone, the SRE reaction begins to occur on the surface of the catalytic wall, while the ethanol in the mainstream is pyrolyzed, which can increase the hydrogen production and heat sink. When the near-wall temperature is higher than 450 °C, the catalytic reforming reaction of EHF begins to occur on the surface of the catalytic wall, and the main reaction gradually transfers from ethanol to EHF. Also, at a higher temperature, the thermal cracking of EHF becomes the main reaction. The effect of water content is to promote the SRE reaction and inhibit the EHF thermal cracking.

3.3. Heat Transfer and Coke Deposition. As demonstrated in Figure 8, the heat transfer process of case 6 can be divided into three stages. At first, the heat transfer coefficient (HTC) increases to a high level, which indicates the enhancement of heat transfer due to the latent heat of the phase transformation of water. Then, EHF also undergoes phase state transition with the increase in temperature, during which the physical properties such as specific heat and thermal conductivity change drastically, resulting in a rapid decrease in HTC. Finally, the HTC increases again due to the heat transfer enhancement caused by endothermic chemical reactions including thermal cracking and catalytic steam reforming of EHF.

The heat transfer process with 10 wt % ethanol addition in case 7 is the same as that in case 6, but the HTC is significantly improved, especially in the low-temperature section from 0.1 to 0.35 m. The maximum value of HTC is increased by 1.96 times. It can be concluded from the above reaction analysis that the heat transfer enhancement by ethanol addition is not only due to the phase change of ethanol but also caused by the endothermic reactions such as pyrolysis and steam reforming of ethanol that began to occur at this temperature.

A comparison of the wall temperature in Figure 8 shows that the heat transfer enhancement caused by ethanol addition reduces the overall wall temperature. The thermal cracking of

https://doi.org/10.1021/acsomega.2c07582
ACS Omega 2023, 8, 6860−6868

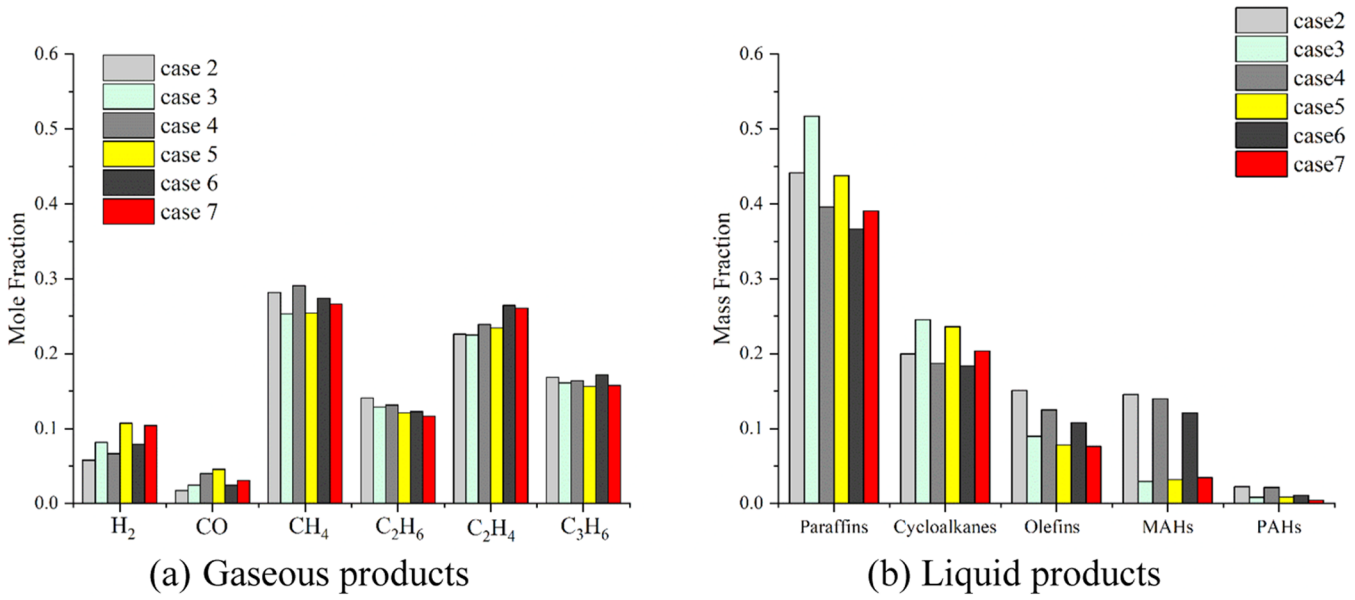

Figure 5. Product distributions at 650 °C.

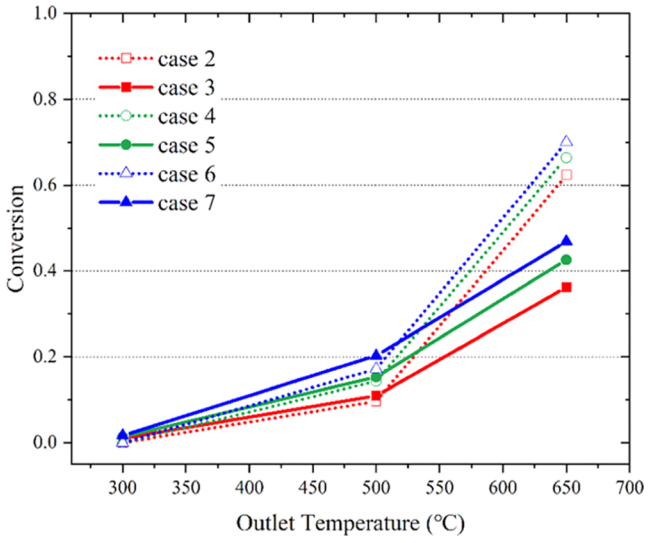

Figure 6. EHF conversion comparison.

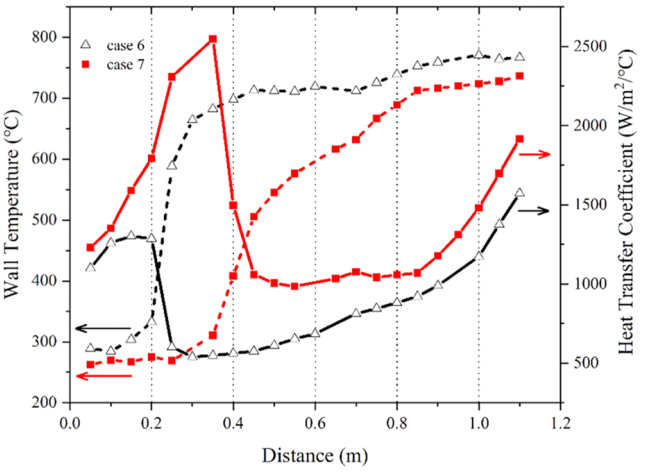

Figure 8. Comparisons of wall temperature and heat transfer coefficient at 650 °C.

EHF occurs only when the temperature exceeds 550 °C. Therefore, under the same inlet and outlet temperature conditions, the wall temperature near the outlet is decreased by about 30 °C, which means the reaction region of thermal cracking is considerably moved backward. Therefore, the thermal cracking of EHF in the reactor is suppressed.

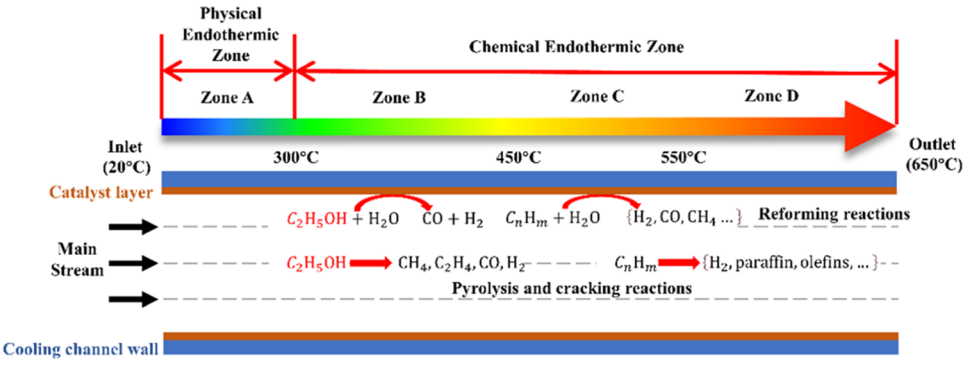

Figure 7. Schematic of main reaction change with temperature.

https://doi.org/10.1021/acsomega.2c07582
ACS Omega 2023, 8, 6860−6868

The coking rates of cases 1, 6, and 7 measured by the TPO method are shown in Figure 9. Our previous research[16] has

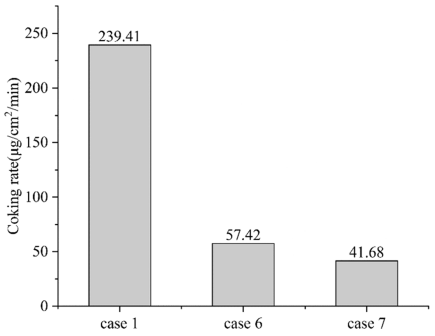

Figure 9. Comparison of coking rates among cases 1, 6, and 7 (from inlet 20 °C to outlet 650 °C, stable conditions for 30 min).

shown that the steam reforming of EHF with catalysts can significantly reduce the coking rate. With 10 wt % ethanol addition, the coking rate further decreases from 57.42 to 41.68 $\mu g/cm^2/min$, which is a relative decrease of 27.41%. The reduction of coking rate is a result of the inhibition of EHF thermal cracking by heat transfer enhancement and the suppression of the coking precursor formation by ethanol addition.

It is generally considered that aromatics have a significant impact on coke deposition. The main pathway for MAH production is the Diels–Alder reaction between alkenes and mono-olefin, such as ethylene and butadiene (eq 10). Then, PAHs are generated by condensation and dehydrogenation reactions of MAHs (eq 11). Also, PAHs are generally considered to be the main precursors in coke deposition.[45,46] In Figure 5b, the mass fractions of MAHs decrease sharply with ethanol addition. Moreover, almost no PAHs were detected in the cases with ethanol addition. Previous studies[32,33,47−49] show that ethanol reactions follow a radical chain reaction mechanism. The hydroxyl group of ethanol adsorbs on the surface of the Ni/Al_2O_3 reforming catalyst and forms $CH_3CH_2O^*$ by the breakage of the O–H bond at first. Then, the chemical bond of ethanol breaks in the order of $-CH_2-$, C–C, and $-CH_3$ as dehydrogenation reaction processes. Large amounts of hydrogen produced by ethanol reactions can inhibit the Diels–Alder reaction to reduce the MAH content, thereby reducing the PAH content, resulting in the reduction of the coking rate. A lower coking rate means a higher temperature condition for fuel to use, so ethanol addition can increase the working temperature upper limit of the active thermal protection system.

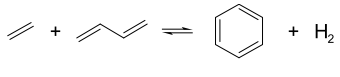

(10)

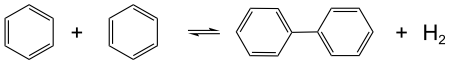

(11)

4. CONCLUSIONS

In this work, ethanol was introduced to the catalytic steam reforming of endothermic hydrocarbon fuel to enhance the thermal protection capability. The characteristics of ethanol-assisted catalytic steam reforming of endothermic hydrocarbon fuel are concluded as follows:

(1) The effects of ethanol addition can be divided into four zones according to the outlet temperature: the physical endothermic zone (<300 °C), the ethanol reactions zone (300–450 °C), the transition zone (450–550 °C), and the EHF reactions zone (>550 °C). The total heat sink can be significantly improved by endothermic reactions of ethanol including dehydration, pyrolysis, and steam reforming. A higher water/ethanol ratio can further increase the chemical heat sink by promoting the SRE reaction. The addition of 10 wt % ethanol at 30 wt % water content can improve the total heat sink by 8–17% at 300–550 °C.

(2) Thermal cracking of EHF is inhibited by ethanol addition. The addition of 10 wt % ethanol enhances heat transfer due to heat absorption by phase transition and chemical reactions. The decrease in overall wall temperature causes the reaction region of thermal cracking to move backward, resulting in the suppression of thermal cracking.

(3) A relative reduction of 27.41% in the coking rate with 10 wt % ethanol addition results from the suppression of the Diels–Alder reaction by the dehydrogenation process in ethanol reactions and the inhibition of EHF thermal cracking by heat transfer enhancement. It is meant that ethanol-assisted catalytic steam reforming of endothermic hydrocarbon fuel can increase the working temperature upper limit of the active thermal protection system.

AUTHOR INFORMATION

Corresponding Author

Lingyun Hou − *Institute for Aero Engine, Tsinghua University, Beijing 100084, China;* orcid.org/0000-0001-9013-9265; Phone: +86 10 62772157; Email: lyhou@tsinghua.edu.cn

Authors

Jiang Guo − *School of Aerospace Engineering, Tsinghua University, Beijing 100084, China*

Mingyu Gao − *School of Aerospace Engineering, Tsinghua University, Beijing 100084, China*

Zekun Zheng − *School of Aerospace Engineering, Tsinghua University, Beijing 100084, China*

Complete contact information is available at: https://pubs.acs.org/10.1021/acsomega.2c07582

Notes

The authors declare no competing financial interest.

ACKNOWLEDGMENTS

The financial assistance provided by the National Science and Technology Major Project (2017-III-0005-0030) is gratefully acknowledged.

REFERENCES

(1) Lander, H.; Nixon, A. C. Endothermic fuels for hypersonic vehicles. *J. Aircraft* **1971**, *8*, 200–207.

(2) Wang, H. Y.; Gao, F.; Li, X. C.; Zhang, H. Thermal protection technology of scramjet combustion chamber. *Aerodyn. Missile J.* **2013**, *10*, 84–87.

(3) Huang, H.; Spadaccini, L.; Sobel, D.In *Endothermic Heat-Sink of Jet Fuels for Scramjet Cooling*, 38th AIAA/ASME/SAE/ASEE Joint Propulsion Conference & Exhibit, 2002.

https://doi.org/10.1021/acsomega.2c07582
ACS Omega 2023, 8, 6860−6868

(4) Xing, Y.; Fang, W. J.; Xie, W. J.; Guo, Y. S.; Lin, R. Thermal Cracking and Heat Sink Measurement of Model Compounds of Endothermic Hydrocarbon Fuels under Supercritical Conditions. *Acta Chim. Sin.* **2008**, *66*, 2243−2247.
(5) Vermeire, F. H.; Aravindakshan, S. U.; Jocher, A.; Liu, M.; Chu, T. C.; Hawtof, R. E.; Van de Vijver, R.; Prendergast, M. B.; Van Geem, K. M.; Green, W. H. Detailed Kinetic Modeling for the Pyrolysis of a Jet A Surrogate. *Energy Fuels* **2022**, *36*, 1304−1315.
(6) Wang, J.; Jin, H.; Gao, H.; Wen, D. Cooling capacity optimization of hydrocarbon fuels for regenerative cooling. *Appl. Therm. Eng.* **2022**, *200*, No. 117661.
(7) Dinda, S.; Vuchuru, K.; Konda, S.; Uttaravalli, A. N. Heat Management in Supersonic/Hypersonic Vehicles Using Endothermic Fuel: Perspective and Challenges. *ACS Omega* **2021**, *6*, 26741−26755.
(8) Mun, J.; Kim, N.; Jeong, B.; Jung, J. Endothermic Cracking of n-Dodecane in a Flow Reactor using Washcoated Activated Carbon on Metal Foam. *ACS Omega* **2022**, *7*, 8518−8525.
(9) Tian, Y.; Qiu, Y.; Hou, X.; Wang, L.; Liu, G. Catalytic Cracking of JP-10 over HZSM-5 Nanosheets. *Energy Fuels* **2017**, *31*, 11987−11994.
(10) Huang, B.; Shrestha, U.; Davis, R. J.; Chelliah, H. K. Endothermic Pyrolysis of JP-10 with and without Zeolite Catalyst for Hypersonic Applications. *AIAA J.* **2018**, *56*, 1616−1626.
(11) Yeh, Y. H.; Tsai, C. E.; Wang, C.; Gorte, R. J. Heat-Flow Measurements forn-Hexane Reactions on H-ZSM-5 and H(Zn)-ZSM-5: Implications for Endothermic Reforming in Hypersonic Aircraft. *Ind. Eng. Chem. Res.* **2017**, *56*, 6198−6203.
(12) Hou, L. Y.; Dong, N.; Sun, D. P. Heat transfer and thermal cracking behavior of hydrocarbon fuel. *Fuel* **2013**, *103*, 1132−1137.
(13) Zhong, F. Q.; Fan, X. J.; Yu, G.; Li, J. G.; Sung, C. J. Thermal Cracking and Heat Sink Capacity of Aviation Kerosene Under Supercritical Conditions. *J. Thermophys. Heat Transfer* **2011**, *25*, 450−456.
(14) Kuranov, A.; Korabelnikov, A.; Mikhailov, A.In *Thermal Protection and Hydrogen Production on Board of the Hypersonic Vehicle*, 8th AIAA/3AF International Space Planes and Hypersonic Systems and Technologies Conference, 2012; pp 867−872.
(15) Kuranov, A. L.; Korabel Nikov, A. V.; Mikhailov, A. M. Conversion of hydrocarbon fuel in elements of thermal protection of a hypersonic flight vehicle. *High Temp.* **2016**, *54*, 397−402.
(16) Gao, M. Y.; Hou, L. Y.; Zhang, X. X.; Zhang, D. R. Coke Deposition Inhibition for Endothermic Hydrocarbon Fuels in a Reforming Catalyst-Coated Reactor. *Energy Fuels* **2019**, *33*, 6126−6133.
(17) Hou, L. Y.; Dong, N.; Ren, Z. Y.; Zhang, B.; Hu, S. L. Cooling and coke deposition of hydrocarbon fuel with catalytic steam reforming. *Fuel Process. Technol.* **2014**, *128*, 128−133.
(18) Hou, L. Y.; Jia, Z.; Gong, J. S.; Zhou, Y. F.; Piao, Y. Heat Sink and Conversion of Catalytic Steam Reforming for Hydrocarbon Fuel. *J. Propulsion Power* **2012**, *28*, 453−595.
(19) Hou, L. Y.; Zhang, X. X.; Ren, Z. Y. Coke suppression of kerosene by wall catalytic steam reforming. *Fuel Process. Technol.* **2016**, *154*, 117−122.
(20) Zheng, Q. C.; Xiao, Z. R.; Xu, J. S.; Pan, L.; Zhang, X. W.; Zou, J. J. Catalytic steam reforming and heat sink of high-energy-density fuels: Correlation of reaction behaviors with molecular structures. *Fuel* **2021**, *286*, 119371.
(21) Feng, Y.; Liu, Y.; Cao, Y.; Gong, K.; Liu, S.; Qin, J. Thermal management evaluation for advanced aero-engines using catalytic steam reforming of hydrocarbon fuels. *Energy* **2020**, *193*, 116738.
(22) Hou, L. Y.; Zhang, D. R.; Zhang, X. X. Interaction between thermal cracking and steam reforming reactions of aviation kerosene. *Fuel Process. Technol.* **2017**, *167*, 655−662.
(23) Liu, S.; Feng, Y.; Chu, Y.; Gong, K.; Cao, Y. Numerical study of catalytic steam reforming of aviation kerosene at supercritical pressures. *Fuel* **2018**, *212*, 375−386.
(24) Li, Z. Y.; Li, D. J.; Huang, G. H.; Wei, H. R. Insights on current development of fuel ethanol. *Chem. Ind. Eng. Prog.* **2013**, *32*, 6−16.
(25) Mason, R. S.; Parry, A. Concerning the thermal decomposition of protonated ethanol in a high pressure ion source and other pyrolysis reactions. *Int. J. Mass Spectrom. Ion Processes* **1991**, *108*, 241−253.
(26) Zhang, M.; Yu, Y. Dehydration of Ethanol to Ethylene. *Ind. Eng. Chem. Res.* **2013**, *52*, 9505−9514.
(27) Wang, J. Studies of Pyrolysis and Cold Plasma of C2−C4 Alcohol Fuels; Ph.D. Thesis, University Of Science and Technology of China: Beijing, China, 2008.
(28) Rossetti, I.; Tripodi, A. Catalytic Production of Renewable Hydrogen for Use in Fuel Cells: A Review Study. *Top. Catal.* **2022**, DOI: 10.1007/s11244-022-01563-z.
(29) Sun, J.; Qiu, X.; Wu, F.; Zhu, W. H2 from steam reforming of ethanol at low temperature over Ni/Y2O3, Ni/La2O3 and Ni/Al2O3 catalysts for fuel-cell application. *Int. J. Hydrogen Energy* **2005**, *30*, 437−445.
(30) Fatsikostas, A. Reaction network of steam reforming of ethanol over Ni-based catalysts. *J. Catal.* **2004**, *225*, 439−452.
(31) Dalena, F.; Giglio, E.; Marino, A.; Aloise, A.; Giorgianni, G.; Migliori, M.; Giordano, G. Steam Reforming of Bioethanol Using Metallic Catalysts on Zeolitic Supports: An Overview. *Catalysts* **2022**, *12*, No. 617.
(32) Sun, S.; Yan, W.; Sun, P.; Chen, J. Thermodynamic analysis of ethanol reforming for hydrogen production. *Energy* **2012**, *44*, 911−924.
(33) Fishtik, I.; Alexander, A.; Datta, R.; Geana, D. A thermodynamic analysis of hydrogen production by steam reforming of ethanol via response reactions. *Int. J. Hydrogen Energy* **2000**, *25*, 31−45.
(34) Huang, G. J.; Zhang, Y. T.; Li, J. B. Thermodynamic Studies on Renewable Hydrogen From Ethanol via Steam Oxidative Reforming. *J. Eng. Thermophys.* **2018**, *39*, 2366−2371.
(35) Comas, J.; Mariño, F.; Laborde, M.; Amadeo, N. Bio-ethanol steam reforming on Ni/Al2O3 catalyst. *Chem. Eng. J.* **2004**, *98*, 61−68.
(36) Gong, J. S.; Yang, Q. T.; Hou, L. Y.; Zhong, B. J. Experimental Study on Pyrolysis Characteristics of Ethanol-Kerosene Mixture. *J. Eng. Thermophys.* **2009**, *30*, 1617−1620.
(37) Xu, G. L.; Yu, C.; Chen, S.; Wu, C. T.; Wang, X. D.; Zhang, T.In *Enhanced Heat Sink by Ethanol Assisted Endothermic Catalytic Cracking of Hydrocarbon Fuels*, 21st AIAA International Space Planes and Hypersonics Technologies Conference, 2017; pp 314−321.
(38) Yang, Z.; Li, G.; Yuan, H.; Liu, G.; Zhang, X. Efficient Coke Inhibition in Supercritical Thermal Cracking of Hydrocarbon Fuels by a Little Ethanol over a Bifunctional Coating. *Energy Fuels* **2017**, *31*, 7060−7068.
(39) Sahoo, S. K.; Rao, P. V. C.; Rajeshwer, D.; Krishnamurthy, K. R.; Singh, I. D. Structural characterization of coke deposits on industrial spent paraffin dehydrogenation catalysts. *Appl. Catal., A* **2003**, *244*, 311−321.
(40) Park, J.; Zhu, R. S.; Lin, M. C. Thermal decomposition of ethanol. I. Ab Initio molecular orbital/Rice−Ramsperger−Kassel−Marcus prediction of rate constant and product branching ratios. *J. Chem. Phys.* **2002**, *117*, 3224−3231.
(41) Park, J.; Xu, Z. F.; Lin, M. C. Thermal decomposition of ethanol. II. A computational study of the kinetics and mechanism for the H +C2H5OH reaction. *J. Chem. Phys.* **2003**, *118*, 9990−9996.
(42) Xu, Z. F.; Park, J.; Lin, M. C. Thermal decomposition of ethanol. III. A computational study of the kinetics and mechanism for the CH3+C2H5OH reaction. *J. Chem. Phys.* **2004**, *120*, 6593−6599.
(43) Peela, N. R.; Kunzru, D. Steam Reforming of Ethanol in a Microchannel Reactor: Kinetic Study and Reactor Simulation. *Ind. Eng. Chem. Res.* **2011**, *50*, 12881−12894.
(44) Mas, V.; Bergamini, M. L.; Baronetti, G.; Amadeo, N.; Laborde, M. A Kinetic Study of Ethanol Steam Reforming Using a Nickel Based Catalyst. *Top. Catal.* **2008**, *51*, 39−48.
(45) Kim, J.; Park, S. H.; Lee, C. H.; Chun, B.-H.; Han, J. S.; Jeong, B. H.; Kim, S. H. Coke Formation during Thermal Decomposition of Methylcyclohexane by Alkyl Substituted C5 Ring Hydrocarbons under Supercritical Conditions. *Energy Fuels* **2012**, *26*, 5121−5134.

https://doi.org/10.1021/acsomega.2c07582
ACS Omega 2023, 8, 6860−6868

(46) Richter, H.; Howard, J. B. Formation of polycyclic aromatic hydrocarbons and their growth to soot—a review of chemical reaction pathways. *Prog. Energy Combust. Sci.* **2000**, *26*, 565−608.
(47) Zanchet, D.; Santos, J. B. O.; Damyanova, S.; Gallo, J. M. R.; Bueno, J. M. C. Toward Understanding Metal-Catalyzed Ethanol Reforming. *ACS Catal.* **2015**, *5*, 3841−3863.
(48) Anil, S.; Indraja, S.; Singh, R.; Appari, S.; Roy, B. A review on ethanol steam reforming for hydrogen production over Ni/Al2O3 and Ni/CeO2 based catalyst powders. *Int. J. Hydrogen Energy* **2022**, *47*, 8177−8213.
(49) Barnard, J. A.; Hughes, H. W. D. The pyrolysis of ethanol. *Trans. Faraday Soc.* **1960**, *56*, 55−63.

https://doi.org/10.1021/acsomega.2c07582
ACS Omega 2023, 8, 6860−6868